Journal of Engg. Research Vol.10 No. (2A) pp. 195-209 DOI: 10.36909/jer.10371

Detection of foreign materials in wheat kernels using regional color descriptors

Neeraj Julka* and A. P. Singh**

** Research Scholar, Department of Electronics and Communication Engineering, SLIET Longowal, 148106, India.*
*** Professor, Department of Electronics and Communication Engineering, SLIET Longowal, 148106, India.*
** Corresponding Author: neerajjulkasliet@gmail.com*

Submitted *:* 11/06/2020
Revised *:* 26/06/2021
Accepted *:* 04/07/2021

ABSTRACT

Present paper reports the development of an automated machine vision system for detection of foreign materials in wheat kernels using regional color descriptors. The said system was executed in the form of an integrated flowing pipeline after having proper choice of different possible alternatives at different stages of image processing. A new type of surface color descriptor is also proposed in this work to define wheat kernel uniquely. The fifteen-element color descriptor is executed after having thorough comparison of six different color spaces, each having 72 separate quantifiable components. The fifteen elements of the proposed color-descriptor, extracted from each segmented region of the sample image, are concatenated in the form of an input to the neural classifier. The neural classifier is trained with Levenberg-Marquardt (LM) learning algorithm to achieve extremely fast convergence. The recognition rate of the executed classifier is found to be more than 99.2% for detection of impurity in unconnected wheat kernels. The results of present investigations are quite promising. The proposed pipeline has potential future in the field of machine vision based quality inspection of wheat and other cereal grains.

Keywords: Color descriptor; Wheat kernel; Neural classifier; Foreign material; Machine vision.

1. INTRODUCTION

India is an agricultural country with 50% of its living population indulged in agriculture for earning livelihood (South Asia , 2020). This amounts to a contribution of 15% of total GDP of India. Such low percentage of GDP indicates that production in agriculture field in India is not remarkable. One of the main reasons of this low production is the use of conventional methods of crop-cultivation including quality inspection of agricultural produce till-date. The increasing demand as well as awareness in consumers has led to improvement in inspection methods of these products. This in turn has necessitated the urgent requirement to develop efficient methods of quality inspection of agricultural produce (Maheshwari, 2013). Grain is one of the important foods in the world as a source of nutrition. Determination of grain type (class) as well as its quality is very crucial at every stage of grain postharvest handling. Traditional manual analysis based grading of grains has many limitations and certain drawbacks. It is highly subjective due to anthropogenic as well as environmental influences on human perception (Maheshwari, 2013). Moreover, such methods are inefficient and time-consuming and very much prone to grading inconsistencies on account of these influences (Maheshwari, 2013). Therefore, need of the hour is to develop an efficient system that is capable of estimating grain quality objectively and rapidly. However, the most useful measure to realize such a system

is to use machine vision based inspection (Luo, Jayas, et. al., 1999; Maheshwari, 2013; Majumdar, et. al., 2000; Mallat, 1989; S. Majumdar, et.al., 2000a; Shibata, et. al., 1996). Many works reported successful application of machine vision in agriculture (Luo et al., 1999; Maheshwari, 2013; Majumdar & Jayas, 2000b, 2000a; Mallat, 1989; S. Majumdar & D. S. Jayas, 2000; Shibata, et al., 1996). These works are documented largely in the area of either agriculture product classification (Abdellaoui, et. al., 2006; Choudhary, et. al., 2008; J. Paliwal, et. al., 1999; Paliwal, et. al., 2003) and/or variety identification (Barker, et. al., 1992; Neuman, et. al., 1989; Sapirsteinr, et. al., 1994). However, impurity detection in wheat in particular is rarely attempted (Luo et al., 1999; Paliwal et al., 2003). However, all these works in respect of reported the use either morphological or textural or color (Majumdar & Jayas, 2000b, 2000a; S. Majumdar & D. S. Jayas, 2000) features or their combination (Abdellaoui et al., 2006; Majumdar et. al.,2000a) for product classification as well as variety identification. In most of these studies, statistical identification techniques are for classification of different varieties of cereal grains using morphological attributes (Majumdar, et. al., 2000, 2000a; 2000b).In other studies (Majumdar & Jayas, 2000b; S. Majumdar & D. S. Jayas, 2000) use of color attributes has also been reported for recognition of grain types. Similarly, combination of morphological and color attributes was also reported in works (Abdellaoui, et al., 2006; Majumdar, et. al., 2000; 2000b; Sapirsteinr, et al., 1994). In majority of the above works, classification of cereal grains is executed by employing intelligent classifiers, either in the form of fuzzy logic based classifier or artificial neural networks based classifier (Chaugule & Mali, 2019) (Visen, et. al., 2002). As far as our knowledge is concerned, artificial neural networks were used only with shape, color and textural attributes. In addition to these methods, wavelet (Barker, et. al., 1992), Fourier (Barker, et al., 1992) and Chebychev Coefficients (Barker, et al., 1992) techniques were also used in the work. The use of slice and aspect ratio parameters (Barker, et. al., 1992) is also documented for the discrimination of Australian wheat varieties. However, all the above reported methods did not study the identification of impurity in mixed sample with wheat grains. Moreover, no machine vision system is reported in the form of a flowing pipeline with each and every component thoroughly researched including correction for uneven illumination automatically. Thus, objective of the present study is to develop algorithm to identify wheat and non-wheat components in mixed samples having wheat and other grains. Moreover, the present work is also concerned with establishment of real time algorithm for quality inspection of unconnected wheat kernels using regional color descriptors. For that purpose, here, a new classification method is proposed for estimation of impurity in mixed wheat samples using artificial neural network. However, the major contribution of the present work includes the development of an intelligent machine vision system for automated quality inspection of wheat using a new type of surface color descriptor of wheat kernels.

2. MATERIALS AND METHODS

In an attempt to develop an efficient machine vision system for quality estimation of wheat kernels, everything had been executed from the scratch in the present work. Every component was executed using an appropriate image processing technique after thorough investigations and that is too after comparing different possible options. Synchronization between different components of the proposed algorithm is also ensured. In this work, supervised machine learning is executed for distinguishing grain particles and impurities. The major contribution in this work is to segment the RGB objects in the given image having binary background. In doing so, region of interest (Bounding Box) is also having binary background with segmented RGB object. The purpose of doing so is to get more accurate quantification of color components as compared to traditional methods of segmentation.

2.1 Experimental Setup

Charged Coupled Device (CCD) containing industrial grade color camera with c-type lens mount is connected through IEEE1394 cable to a software-driven image-grabber interface that is fixed in PCI slots of a desktop personal computer for image acquisition. Industrial standard LED lights are used for attaining uniform illumination over the

image area. Color camera is firmly mounted on a specially designed iron stand at a fixed height for its easy movement in the horizontal and vertical directions as well as fixed angle of viewing. For the preparation of wheat kernel image dataset, black color is chosen as the background in order to reduce the shadow effect of grains. Images were taken having mono-color background (black). These are uniformly illuminated with sufficient lighting. MATLAB version R-2019a having Image Acquisition, Image Processing and Neural Network Toolboxes is installed in the personal computer for developing Graphical User Interface (GUI) of the proposed pipeline in its AppDesigner environment.

2.2 Preparation of Image Dataset

No standard image dataset of wheat kernels as well as impurity in question is available for these investigations. In order to benchmark the results of present investigations, sample image data containing wheat and non-wheat (impurity) components were prepared. Samples of nine verities of wheat crop, grown over different regions of North India, were acquired from Akal Seed Farm, Mastuana Sahib, District Sangrur, Punjab, India. These varieties included PBW-550, PBW-550 Unat, WH-1105, WH-542, PBW-725, HD-3086, HD-2329, HD-2967 and PBW-677 as categorized by the concerned seed farm. The investigations were conducted with different types of non-wheat components including Barley, Oat, White Chic-pea, Black Chic-pea, Corn, Chaff, Straw and Stones. In this way, 40 number of sample images, each having nearly 30 number of wheat kernels, mixed from above mentioned nine varieties, are acquired in a single frame and stored in the hard disk of Desktop PC. While acquiring images, placement of kernels and impurity elements in a frame was done manually to avoid touching of the same with each other. In this way, an image set was acquired that contained total 1235 wheat kernels. Similarly, another image set was also acquired having a mixture of seven impurities (foreign materials) as detailed above and wheat kernels. Thus, total data set prepared for the present investigations contained 1235 wheat kernels and 193 impurity elements (foreign materials).

2.3 Proposed Pipeline

Acquired images are preprocessed to remove noise and illumination variants. Each grain/impurity is extracted as a separate segment through segmentation. Separate segments are tested on trained neural model to classify it as grain or impurity. Then, accordingly, quality estimate of sample is predicted. Sample is an approximate representative of heap. In order to model this assumption, a number of different samples were taken. Average quality estimate of all sampled segments is predicted. Digital filter is employed to remove noise and smoothen it further. Image is further sharpened to enhance edges of overlapping grains as well as making kernel touching borders (if any) cleared and the same has been taken into account while computing overall purity of the given sample. Image is converted to binary image using threshold. Binarized image obtained so has a lot of dots and overlapping particles. Morphological opening is used to remove stray dots and open up slightly overlapping particles. Threshold based Otsu's method of segmentation is proposed to segment each particle in the given image. This step takes binary image as input and provides clusters of grains as output. All the connected components in binary image are traced. Also, all the components with pixel area less than the specified threshold are removed from the acquired image. Each remaining component is a kernel or impurity segment. The above steps are used to extract segments from image. In this way, complete flowing pipeline is developed as illustrated in Figure 1. The different sixteen stages of image processing indicated in Figure 1 are executed sequentially. These seventeen modules are integrated meticulously one after the other to achieve proper segmentation of all the required objects in the given image for further processing. However, the ultimate aim of these integrated modules is to get binary background of the sample image with RGB object embedded over it.

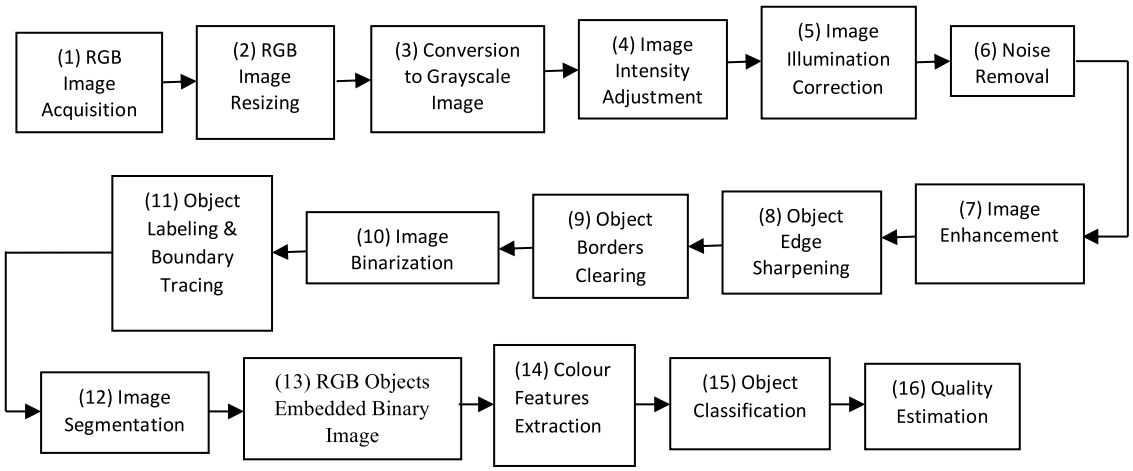

Figure 1. Block Diagram of the Proposed Pipeline.

2.3.1 Color Components Extraction & Quantification

After segmentation of RGB objects from the image with binary background, next step is to convert RGB object to six different color spaces. An algorithm is written in MATLAB to achieve this specific task and the same is also integrated as one of the constituting modules of the flowing pipeline. After getting the given image properly segmented, the next step is the extraction of color features from the segmented image. For doing so, the first step is to get proper labeling of different objects in the image. Then, the algorithm was executed for proper counting of the total objects in the same. The major task in the present problem is the extraction of features from wheat and non-wheat components one by one covering the complete image. Six different color spaces (Gonzalez, et. a;., 2004) are chosen for this purpose. Out of these, RGB color space is used extensively (Majumdar, et. al., 2000b) to represent color attributes of cereal grains including wheat. This specific task is also executed by the above-mentioned algorithm in the proposed pipeline. However, the present work also reports the extraction of color features from other five important color spaces including HV, HIS, NTSC (YIQ), YCbCr and CMY (Gonzalez, et al., 2004). Out of these, HSV color space is also used in some works on different cereal grains. However, the remaining four color spaces have been rarely investigated. An RGB color image is a three-dimensional array of color pixels in which each color pixel is considered as a triplet of red, green and blue components. Such a model is classified into two types including linear RGB color space and nonlinear RGB color space. The transformation from linear to nonlinear values is defined below:

$$R' = \begin{cases} 4.5R & if\ R \le 0.018 \\ 1.099R^{\frac{1}{\gamma C}} - 0.099 & otherwise \end{cases} \quad (1)$$

$$G' = \begin{cases} 4.5G & if\ G \le 0.018 \\ 1.099G^{\frac{1}{\gamma C}} - 0.099 & otherwise \end{cases} \quad (2)$$

$$B' = \begin{cases} 4.5B & if\ G \le 0.018 \\ 1.099B^{\frac{1}{\gamma C}} - 0.099 & otherwise \end{cases} \quad (3)$$

where γC is the gamma factor of the camera. The value of γC that is commonly used in video cameras is 1/145 (≈2. 22). The digital values of the image pixels acquired from the object and stored within a camera are the R'B'G' values usually converted to the range of 0 to 255. Three bytes are then required to represent the three components, R', G' and B' of a color image pixel with one byte for each component. From nonlinear to linear conversion, the transformation (Gonzalez, et. al., 2004) is defined below.

$$\mathrm{R} = \begin{cases} \frac{\mathrm{R}'}{4.5} & if\ \mathrm{R}' \leq 0.018 \\ \left(\frac{\mathrm{R}'+0.099}{1.099}\right)^{\gamma \mathrm{D}} & \text{otherwise} \end{cases} \tag{4}$$

$$\mathrm{G} = \begin{cases} \frac{\mathrm{G}'}{4.5} & if\ \mathrm{G}' \leq 0.018 \\ \left(\frac{\mathrm{G}'+0.099}{1.099}\right)^{\gamma \mathrm{D}} & \text{otherwise} \end{cases} \tag{5}$$

$$\mathrm{B} = \begin{cases} \frac{\mathrm{B}'}{4.5} & if\ \mathrm{B}' \leq 0.018 \\ \left(\frac{\mathrm{B}'+0.099}{1.099}\right)^{\gamma \mathrm{D}} & \text{otherwise} \end{cases} \tag{6}$$

The value of the power function, γD, is known as the gamma factor of the display device. However, normal display devices have γD in the range of 2.2 to 2.45. In the HSV color space, H stands for hue (tint), S for saturation (shade) and V for value (tone) and this color space is usually used to select colors for paints or inks from a color wheel or palette. However, HSV space is closer to RGB space to the way in which humans experience and describe color situations. Similarly, in HIS color space, H stands for hue, I for intensity and S for saturation values. In this space, H component of each RGB pixel of the given color image is computed using following equation:

$$H = \begin{cases} \theta if B \leq G \\ 360 - \theta if B > G \end{cases} \quad \text{where, } \theta = \left\{ \frac{\frac{1}{2}[(R-G)+(R-B)]}{[(R-G)^2+(R-B)(G-B)]^{\frac{1}{2}}} \right\} \tag{7}$$

Also, saturation component of each RGB pixel is computed from the following expression:

$$S = 1 - \frac{3}{(R+G+B)}[\min(R,G,B)] \tag{8}$$

On similar way, intensity component is computed from the following equation:

$$I = \frac{1}{3}(R+G+B) \tag{9}$$

The fourth color space, YIQs space, is used usually in television broadcasting and advantage of this space lies in the fact that gray scale information is separated from color data in this space. Therefore, same signal is used both for monochrome as well as color transmission. In this format, image data consists of three components including luminance (Y), hue (I) and saturation (Q) and the same is related to RGB components by the following mathematical expression:

$$\begin{bmatrix} Y \\ I \\ Q \end{bmatrix} = \begin{bmatrix} 0.299 & 0.587 & 0.114 \\ 0.596 & -0.274 & 0.322 \\ 0.211 & -0.523 & 0.312 \end{bmatrix} \begin{bmatrix} R \\ G \\ B \end{bmatrix} \tag{10}$$

The fifth color space, YCbCr color space, is used widely in digital video. In this format, luminance information is represented by a single component, Y, and color information is stored as two color-difference components, Cb and Cr. This color space is related to RGB color space by the following expression:

$$\begin{bmatrix} Y \\ Cb \\ Cr \end{bmatrix} = \begin{bmatrix} 16 \\ 128 \\ 128 \end{bmatrix} + \begin{bmatrix} 65.481 & 128.553 & 24.966 \\ -37.797 & -74.203 & 112.0002 \\ 112.000 & -93.786 & -18.214 \end{bmatrix} \begin{bmatrix} R \\ G \\ B \end{bmatrix} \tag{11}$$

In the last color space, that is, CMY color space, cyan, magenta and yellow are the secondary colors of light. These are also known as secondary color of pigments. For example, when a surface coated with cyan pigment is illuminated with white light, no red light is reflected from the surface. Here, the cyan pigment subtracts red light from reflected white light, which itself is composed of equal amounts of red, green and blue lights. The conversion is performed using following equation:

$$\begin{bmatrix} C \\ M \\ Y \end{bmatrix} = \begin{bmatrix} 1 \\ 1 \\ 1 \end{bmatrix} - \begin{bmatrix} R \\ G \\ B \end{bmatrix} \tag{12}$$

Four color space quantitative components like Average, Standard Deviation, Variance and Coefficient of Variance are extracted from color channels in RGB, NTSC, YCbCr, HSV, CMY and CMYK, and HIS color spaces (Basati et al., 2018; Mallick & Mohanty, 2020). These components are computed in each case using formulae as documented in Table 1:

Table 1. Mathematical Expression for the Computation of Color Space Components (Majumdar, et. al., 2000b, 2000a)

Color Space Component Quantifier	Mathematical Expression
Average	$\mu = \frac{1}{N}\sum_{i=0}^{N-1} x\,i$ (13)
Standard Deviation	$\sigma = \sqrt{\frac{1}{N}\sum_{i=1}^{N}(xi - \mu)^2}$ (14)
Variance	$\sigma^2 = \frac{1}{N}\sum_{i=1}^{N}(xi - \mu)^2$ (15)
Coefficient of Variation	$CoV = \frac{StandardDeviation}{Average} \times 100$ (16)

2.3.2 Execution of Neural Classifier

One of the other major tasks in the proposed method is to develop of an Artificial Neural Network (ANN) based classifier for recognition of foreign material in wheat kernels using their color attributes. The neural classifier executed in the present work for classification of wheat and non-wheat components comprised of three layers. The input layer is composed of 15 neurons, reflecting the color space components (X_R) and in the present case R is 15. In order to train the proposed neural classifier, a set of images having predefined wheat and non-wheat components was acquired. During training, the connection weights of the neural network were initialized with some random values. Neural classifier performs a nonlinear functional mapping from the past observations (X_{t-1}, X_{t-2}, …, X_{t-p}) to the future value, X_t, that is,

$$X_t = f\left(X_{t-1}, X_{t-2}, \ldots, X_{t-p}\right) + et \tag{17}$$

where f is a function determined by the network structure and connection weights. Thus a neural network is equivalent to a nonlinear autoregressive network. The proposed neural classifier illustrated in Figure 2 was executed with parameters indicated in Table-2. S is number of neurons in the hidden layer and in the present case, it is 10. The output in the present case is either 0 or 1, i.e. weather a given component is wheat or non-wheat. In order to train the neural network, a set of training wheat and non-wheat components are acquired. The training samples in the training set were input to the neural network classifier in random order and connection weights were adjusted using Levenberg-Marquadt algorithm (Khehra, et. al., 2016; Singh, et. al., 2005; Sivia, et. al., 2013). This process was repeated until the mean square error (MSE) fell below a predefined tolerance level or the maximum number of iterations is achieved. When the network training was finished, the network was validated with test data set and detection accuracy was computed. Table-2 indicates the design and performance parameters of the executed neural estimator.

Table 2. Design and Performance Parameters of the Proposed Neural Estimator.

Training Algorithm	Network Topology	Neuron Activation		Number of Neurons			Achieved Performance		
		Hidden Layer	Output layer	Input Layer	Hidden Layer	Output Layer	Epochs	MSE	Gradient
Levenberg Marquardt Back-propagation	Multilayer Feed-Forward	Tansigmoidal	Linear	15	10	1	11	3.6563×10^{-9}	2.5668×10^{-8}

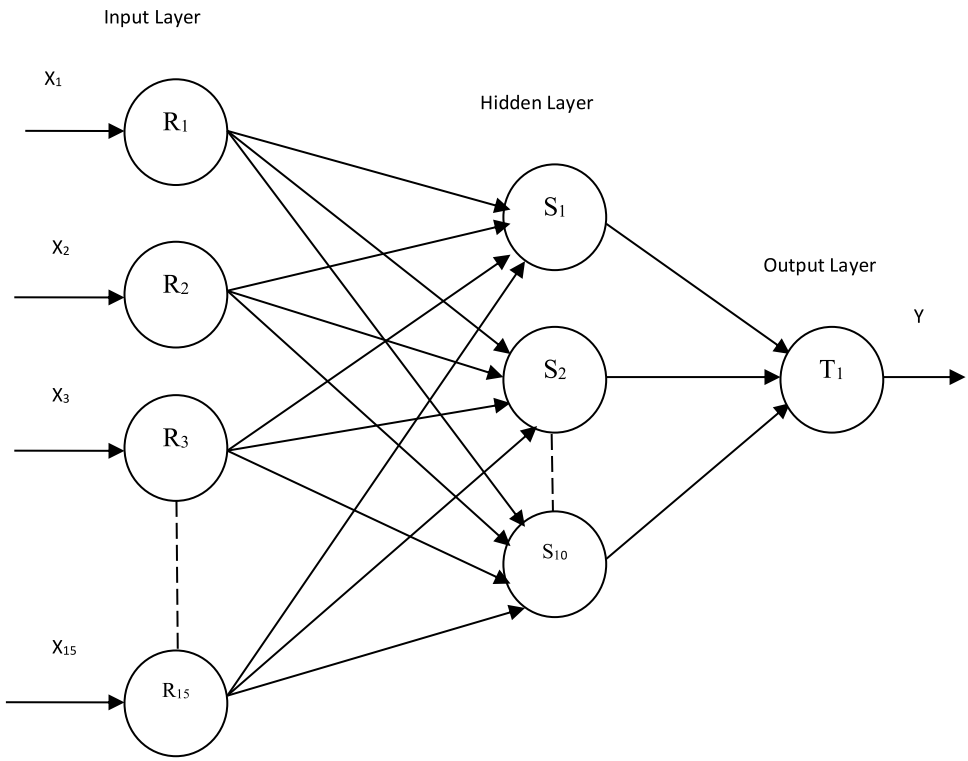

Figure 2. Proposed Neural Classifier.

3. RESULTS AND DISCUSSION

Performance of the proposed pipeline in extracting RGB object with binary image background is illustrated in Figure 3. In this segmentation, the bounding box contains the RGB object. The regions of the Bounding Box lying outside the RGB object are having binary background. This has been done to achieve uniform surface of the bounding box outside the region occupied by the RGB object. This has led to estimation of more accurate RGB components. While converting the RGB object to other spaces, the same feature of uniform background will be propagated leading to accurate estimation of other color spaces of the RGB objects. Such type of color component extraction has not been reported earlier. In traditional methods reported till date, color image segmentation is done to segment the RGB object for extraction of RGB components. However, this type of conventional segmentation does not have the uniform region of the bounding box outside the region occupied by the RGB object. Hence, the quantification of RGB components is not as accurate as is obvious from the proposed technique. Proceeding similarly, as stated above, this module segment all the RGB objects in the given image for extraction of RGB components one by one as illustrated in Figure 4. On examination of the results indicated in Figure 4, the performance of the segmentation module of the proposed pipeline is found to be 100% accurate in segmenting the different RGB objects as confirmed from automatic as well as manual counting and position placement of the objects in the given image. Exact counting as well as correct position placement the different objects (kernels and impurity) in the given image by the proposed algorithm confirms the performance of the individual image processing components of the integrated pipeline effectively.

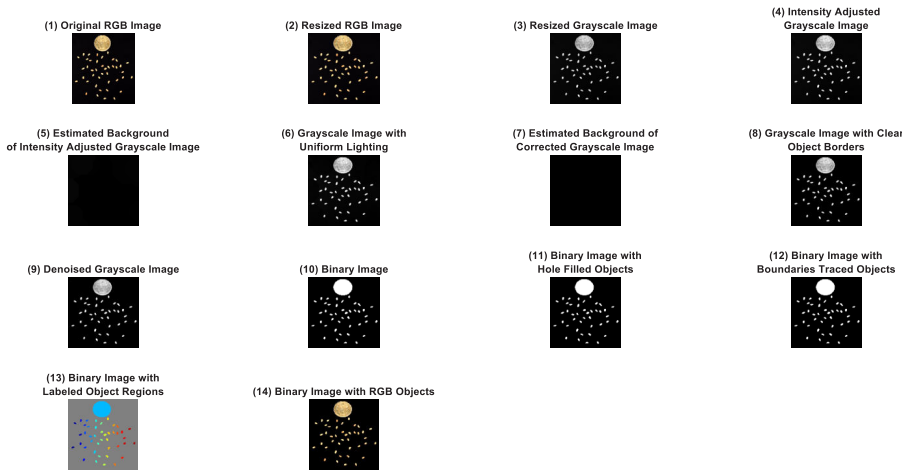

Figure 3. Performance of the proposed pipeline in segmenting RGB object with binary image background.

Figure 4. Segmentation of different RGB objects in the given wheat image.

Next module of the pipeline as stated earlier, convert the RGB object with binary background to different color spaces. A total of six color spaces are executed. From, each color space, three components are extracted quantitatively to describe the color signature of each component in the image. In fact, such powerful quantification has not been reported in the literature so far to describe the wheat kernel as well as seven of the impurity elements. These signatures

describe uniquely each object in the image. In order to assess statistically, average, standard deviation, variance and co-variance of each of the eighteen components of the wheat kernel constitute 72 component powerful features of the same. This powerful 72-dimensional signature of the constituting object describes uniquely the finger print of the object. From this finger, further neural classified is trained to make a distinction between wheat and non-wheat components in the given image. Figure 5 illustrates the performance of the algorithm executed for extraction of different color components quantitatively from Segmented RGB Wheat Kernel with Binary Background.

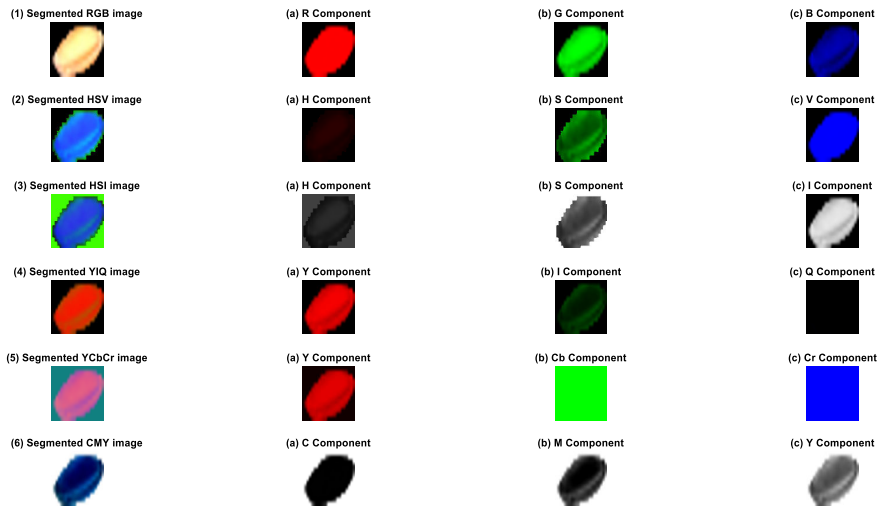

Figure 5. Different Colour Components Extracted from Segmented RGB Wheat Kernel with Binary Background.

Table-3 indicates the quantitative estimate of the 15 regional color descriptors out of a total of 72 of the grain as well as non-grain components chosen in the present investigations. These 15 regional color descriptors describe the color attribute wheat and non-wheat components quantitatively in different color spaces in computer environment. These quantitative descriptors indicate quality estimate of wheat and non-wheat component. Average, Standard deviation, variance and coefficient of variance values of these 15 color descriptors of the wheat and non-wheat components, indicated in Table-3, constitute the input vector of the proposed neural classifier. Regional color descriptors of wheat and non-wheat components clearly define the feasibility of distinction between different wheat and non-wheat components in the image for identification. However, in order to execute proposed classifier effectively, determination of distinction possibility is required invariably. The capability of making a distinction between wheat and non-wheat element by the proposed absolute color space component of both the classes selected for the execution of proposed neural estimator is also illustrated in Figure 6.

Table 3. Absolute Color Space Component of Grain and Non-grain Particles.

S.No.	Model	Wheat		Oat	Barley	White Chickpea	Black Chickpea	Chaff	Straw	Stone
1	RGB	Average R	154.1245	135.4647	118.9321	162.6667	138.8184	128.1137	60.4288	143.7651
2		Average G	133.0408	100.4244	92.4008	117.6443	53.7112	96.4985	49.7894	85.3164
3		Average B	88.7763	70.3452	68.7700	85.2252	25.7193	70.4507	40.8842	64.1507
4		STD in G	86.8656	78.2172	68.1834	73.6000	35.0215	68.7675	55.6071	56.0469
5		Variance in G	7545.6	6117.2	4649	5417	1226.5	4729	3092.1	3141.3
6	HSV	Average H	0.0787	0.0534	0.0465	0.0503	0.0294	0.0446	0.0226	0.0313
7		STD in H	0.0504	0.0475	0.0322	0.0308	0.0180	0.0316	0.0258	0.0209
8	YIQ	Average Y	0.5267	0.4356	0.3829	0.4996	0.2979	0.4038	0.2037	0.3936
9		STD in Y	0.3412	0.3176	0.2816	0.3108	0.1903	0.2871	0.2264	0.2552
10		Variance in Q	9894.3	7909.914	6998.5	8133.6	7428	9654	7549.7	5915.8
11	YCbCr	Average Y	131.3360	101.3456	99.8585	125.4218	81.2421	104.4426	60.6219	102.2094
12		STD in Y	75.8269	60.9474	57.6534	72.4123	46.9051	60.3000	35.0000	59.0106
13		Variance in Y	5749.7	3714.586	3323.9	5243.5	2200.1	3636.1	1225	3482.3
14	CMY	STD in M	0.4082	0.3244	0.3563	0.3287	0.1643	0.3503	0.3424	0.2651
15		COV in M	85.357	71.04687	55.878	61.017	20.82	56.356	42.549	39.845

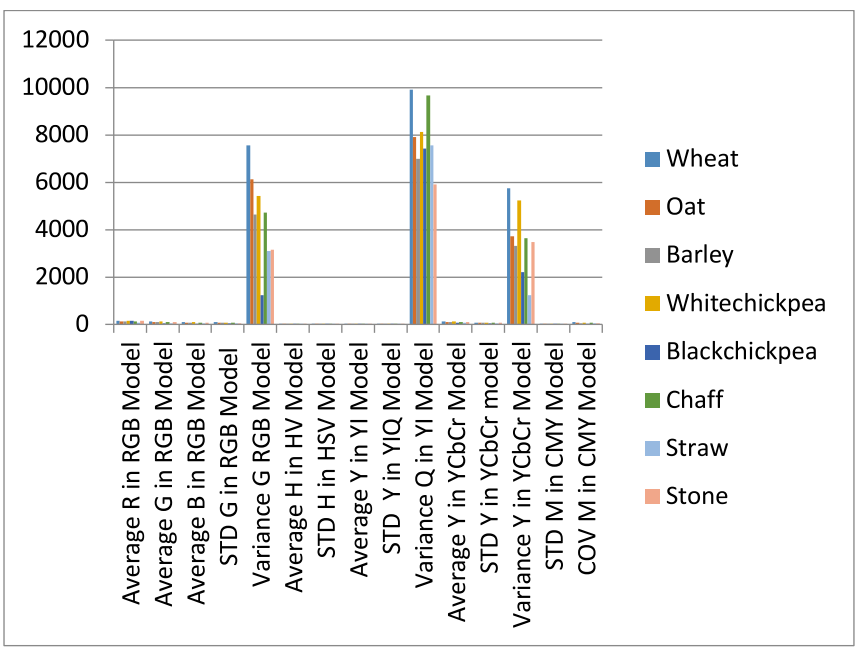

Figure 6. Absolute Color Space Component of Grain and Non-grain Particles.

The performance of the proposed machine vision system is tabulated in Table-4. The non-wheat components investigated in the present study include barley, oat, black-chickpea, white-chickpea, chaff, straw and stone. The neural classifier trained with Levenberg-Marquardt learning is executed in MATLAB environment using its Neural Network Toolbox. However, the proposed neural classifier is executed after having proper training and testing phases executed in MATLAB. For doing so, neural classifier executed in MATLAB environment itself takes 85% of image data for training of the classifier, whereas remaining 15% data is used for testing purposes. Figure 7 shows the Confusion Matrices obtained by using Proposed Neural Classifier. These matrices include Training Confusion Matrix, Validation Confusion Matrix, Testing Confusion Matrix and all-confusion matrix. Results validate the excellent performance of the proposed neural classifier. As confirmed from these confusion matrices, the object recognition rate for impurity (foreign) elements is found to be 100%.

It is also established that, wheat kernels are detected with an accuracy of 99.2%. It is further revealed that 0.8% percent of wheat kernels have been detected as impurity elements. On further analysis of the specific results, it is found that 0.8% of the wheat kernels are recognized as white-chickpeas by the proposed neural classifier. This is due to the reason that white-chick pea is having almost similar surface color as that of wheat kernels. In this way, overall detection accuracy of the proposed machine vision system is found to be 99.2%. The attainment of such a high value of detection accuracy confirms the effectiveness of the proposed system.

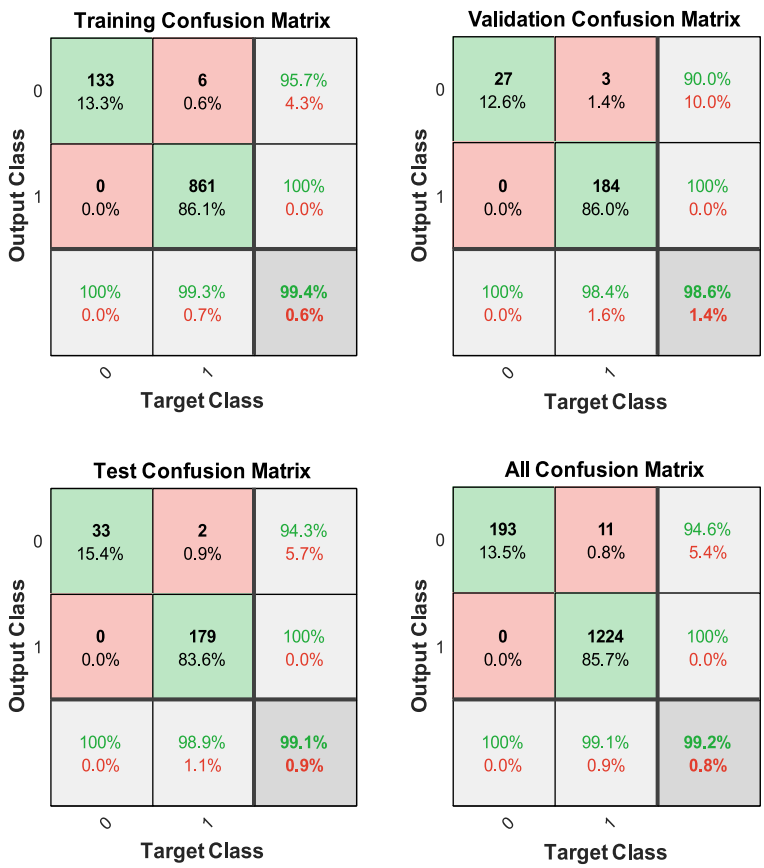

Figure 7. Confusion Matrix obtained by using Proposed Neural Classifier.

Table 4. Detection Accuracy of the Proposed Neural Classifier.

Estimator	Confusion Matrix				Detection Accuracy
Neural Classifier		Wheat Kernels	Impurity		99.2%
	Wheat Kernels	1224	0	1224	
	Impurity	11	193	204	
		1235	193	1428	

4. CONCLUSION

The presented study was conducted to develop an integrated machine vision system in the form of a flowing pipeline for detection of foreign materials in wheat kernels using regional color descriptors. The main objective of the study was to determine the discriminating ability of the proposed color attributes for identification of wheat and non-wheat components in a sample of unconnected wheat kernels as well as detection of foreign materials in the same. A new type of surface color descriptor is also developed in this work to define wheat kernel uniquely. The novelty of the present work is to demonstrate the use of an integrated flowing pipeline having neural classifier as an effective decision maker trained with a reduced number of surface color attributes of wheat kernels. Total error attained with the executed neural classifier is less than 0.8% for detection of impurity in unconnected wheat seeds. Thus, the overall detection accuracy of the executed flowing pipeline is found to be higher than 99.2%. Moreover, the use of black color cloth surface chosen as the image viewing platform for placing wheat and non-wheat components ensured the reduction of grain shadow effect considerably. This study is also relevant to realize the development of comprehensive machine vision system for automated quality inspection of wheat and other cereal grains in future online trading using Internet of Things (IoT). The work is under further progress in this direction.

ACKNOWLEDGMENT

The authors wish to thank Sant Longowal Institute of Engineering (SLIET), Longowal-148106, Sangrur, Punjab, India, for permitting to carry out the present work. Thanks are also due to the Head, Department of Electronics and Communication Engineering, SLIET, Longowal, for extending excellent lab facilities in its Machine Vision and Motion Control Lab.

REFERENCES

Abdellaoui, M., Douik, A., & Annabi, M. (2006). Hybrid method for cereal grain identification using morphological and color features. *Proceedings of the IEEE International Conference on Electronics, Circuits, and Systems*, 870–873. https://doi.org/10.1109/ICECS.2006.379927

Barker, D. A., Vuori, T. A., Hegedus, M. R., & Myers, D. G. (1992). The use of ray parameters for the discrimination of australian wheat varieties. *Plant Varieties & Seeds*, *5*(1), 35–45.

Barker, D. A., Vuori, T. A., & Myers, D. G. (1992). The use of slice and aspect ratio parameters for the discrimination of australian wheat varieties. *Plant Varieties & Seeds*, *5*(1), 47–52.

Basati, Z., Rasekh, M., & Abbaspour-Gilandeh, Y. (2018). Using different classification models in wheat grading utilizing visual features. *International Agrophysics*, *32*(2), 225–235. https://doi.org/10.1515/intag-2017-0008

Chaugule, A., & Mali, S. N. (2019). Evaluation of Texture and Shape Features for Classification of Four Paddy Varieties. *Journal of Engineering (United Kingdom)*, *2019* https://doi.org/10.1155/2019/617263

Choudhary, R., Paliwal, J., & Jayas, D. S. (2008). Classification of cereal grains using wavelet, morphological, colour, and textural features of non-touching kernel images. *Biosystems Engineering*, *99*(3), 330–337. https://doi.org/10.1016/j.biosystemseng.2007.11.013

Gonzalez, R. C., Woods, R. E., & Eddins, S. L. (2004). Digital Image Processing Using Matlab - Gonzalez Woods & Eddins.pdf. In *Education* (Vol. 624, Issue 2, p. 609). https://doi.org/10.1117/1.3115362

Khehra, B. S., & Pharwaha, A. P. S. (2016). Classification of clustered microcalcifications using MLFFBP-ANN and SVM. *Egyptian Informatics Journal*, *17*(1), 11–20. https://doi.org/10.1016/j.eij.2015.08.001

Luo, X., Jayas, D. S., & Symons, S. J. (1999). Identification of damaged kernels in wheat using a colour machine vision system. *Journal of Cereal Science*, *30*(1), 49–59. https://doi.org/10.1006/jcrs.1998.0240

Maheshwari, C. V. (2013). MACHINE VISION TECHNOLOGY FOR ORYZA SATIVA L.(RICE). In *International Journal of Advanced Research in Electrical, Electronics and Instrumentation Engineering* (Vol. 2).

Majumdar, S., & Jayas, D. S. (2000a). Classification of cereal grains using machine vision: IV. Combined morphology, color, and texture models. *Transactions of the American Society of Agricultural Engineers*, *43*(6), 1689–1694. https://doi.org/10.13031/2013.3069

Majumdar, S., & Jayas, D. S. (2000b). Classification of Cereal Grains Usingmachine Vision: Ii. Colormodels. *Transactions of the ASAE*, *43*(6), 1677–1680.

Mallat, S. G. (1989). A Theory for Multiresolution Signal Decomposition: The Wavelet Representation. *IEEE Transactions on Pattern Analysis and Machine Intelligence*, *11*(7), 674–693. https://doi.org/10.1109/34.192463

Mallick, P. K., & Mohanty, B. . (2020). Identification and Classification of Similar Looking Food Grains. *International Journal Of Recent Advances in Engineering & Technology*, *08*(04), 21–25. https://doi.org/10.46564/ijraet.2020.v08i04.006

Neuman, M. R., Sapirstein, H. D., Shwedyk, E., & Bushuk, W. (1989). Wheat grain colour analysis by digital image processing I. Methodology. *Journal of Cereal Science*, *10*(3), 175–182. https://doi.org/10.1016/S0733-5210(89)80046-3

Paliwal, J., Shashidhar, N. S., & Jayas, D. S. (1999). Grain kernel identification using kernel signature. *Transactions of the American Society of Agricultural Engineers*, *42*(6), 1921–1924. https://doi.org/10.13031/2013.13357

Paliwal, J., Visen, N. S., Jayas, D. S., & White, N. D. G. (2003). Cereal grain and dockage identification using machine vision. *Biosystems Engineering*, *85*(1), 51–57. https://doi.org/10.1016/S1537-5110(03)00034-5

S. Majumdar, & D. S. Jayas. (2000). CLASSIFICATION OF CEREAL GRAINS USING MACHINE VISION: I. MORPHOLOGY MODELS. *Transactions of the ASAE*, *43*(6), 1669–1675. https://doi.org/10.13031/2013.3107

Sapirsteinr, H. D., Kohlerl', J. M., Sapirstein, H. D., & And Kohler, J. (n.d.). *Physical uniformity of graded railcar and vessel shipments of Canada Western ned Spring wheat determined by digital image analysis*.

SHIBATA, T., IWAO, K., & TAKANO, T. (1996). Evaluating Tomato Ripeness Using a Neural Network. *Shokubutsu Kojo Gakkaishi*, *8*(3), 160–167. https://doi.org/10.2525/jshita.8.160

Singh, A. P., Kamal, T. S., & Kumar, S. (2005). Development of ANN-based virtual fault detector for Wheatstone bridge-oriented transducers. *IEEE Sensors Journal*. https://doi.org/10.1109/JSEN.2005.845202

Singh Sivia, J., Partap Singh Pharwaha, A., & Singh Kamal, T. (2013). ANALYSIS AND DESIGN OF CIRCULAR FRACTAL ANTENNA USING ARTIFICIAL NEURAL NETWORKS. In *Progress In Electromagnetics Research B* (Vol. 56).

***South Asia :: India — The World Factbook - Central Intelligence Agency*. (n.d.).**Retrieved

April 27, 2020, from https://www.cia.gov/library/publications/the-world-factbool/geos/in.html

Visen, N. S., Paliwal, J., Jayas, D. S., & White, N. D. G. (2002). Specialist neural networks for cereal grain classification. *Biosystems Engineering*, *82*(2), 151–159. https://doi.org/10.1006/bioe.2002.0064